Ultrasmall metal-organic framework Zn-MOF-74 nanodots: size-controlled synthesis and application for highly selective colorimetric sensing of iron (III) in aqueous solution

Jiuhai Wang[†], Yadi Fan[†], Hang-wei Lee[‡], Changqing Yi[§], Changming Cheng[†,£], Mo Yang[*,†]

† Department of Biomedical Engineering, PolyU Shenzhen Research Institute, the Hong Kong Polytechnic University, Hong Kong SAR, China

£ Institute of Nuclear Physics and Chemistry, China Academy of Engineering Physics (CAEP), Mianyang, China

‡ Department of Applied Biology and Chemical Technology, the Hong Kong Polytechnic University, Hong Kong SAR, China

§ Key Laboratory of Sensing Technology and Biomedical Instruments (Guangdong Province), School of Biomedical Engineering, Sun Yat-Sen University, Guangzhou, China.

*E-mail: mo.yang@polyu.edu.hk

KEYWORDS: metal-organic framework, nanodot, zero-dimensional, colorimetric sensing, metal ion detection

ABSTRACT

Here, a novel colorimetric sensing platform for highly selective detection of Fe^{3+} in aqueous solutions was developed based on zero-dimensional Zn-MOF-74 [Zn_2(DOBDC), DOBDC=2,5-dihydroxyterephthalic acid] nanodots. The first ultrasmall Zn-MOF-74 nanodots with the average size within 10 nm was successfully synthesized by manipulating the initial conditions with a diluted material system. It is found that the ultrasamll MOF nanodots have a highly selective interaction with Fe^{3+} and showed a specific blue colorimetric change in aqueous solution. The highly dispersive nature in aqueous solution and high surface-to-volume ratio help MOF-74 nanodots closely interact with the targeted Fe^{3+} ions with a low limit of detection of 1.04 μM and a fast response within seconds. Finally, we demonstrate that the selective Fe^{3+} sensing mechanism of Zn-MOF-74 nanodots is due to the selective framework disruption and the formation of Fe-DOBDC salt complex with blue color. It is the first report of nanoscale MOF based colorimetric Fe^{3+} sensor with low limit of detection (LOD) comparable even to fluorescent MOF based Fe^{3+} sensors, which could be easily observed by naked-eye without expensive fluorescence apparatuses. The good colorimetric stability in aqueous environment, low limit of detection, rapid response and nanosize nature enable this MOF nanodot to be a good Fe^{3+} sensing probe for biological and environmental sensing applications.

1. INTRODUCTION

Fe^{3+} ion is one of the most essential elements in biological systems due to its crucial role in a variety of biochemical processes such as oxygen storage and transport in blood.[1] Various physiological disorders including anemia, skin ailments, insomnia, dysfunction of organs and even cancers are found to be associated with the abnormal level of Fe^{3+}.[2] Therefore, sensitive and

selective detection of Fe^{3+} is of high importance for the surveillance of human health. Traditional techniques for Fe^{3+} ion detection include chromatography,[3] inductively coupled plasma mass spectrometry (ICP-MS)[4] and atomic absorption spectroscopy,[5] which suffer from the complex operation, bulky equipment and high cost. Therefore, it is of high importance to develop a rapid, simple and low-cost approach for sensitive detection of Fe^{3+} ion.

Metal-organic framework (MOF), also called coordination polymers, are a class of inorganic and organic hybrid materials formed by self-assembly of metal ions or clusters and organic bridging ligands. Since the term "MOF" was firstly used by Yaghi in 1995,[6] researchers have achieved significant progress in this field, from rational design[7] and synthesis with predictable structures and functionality[8] to applications such as gas storage/separation, catalysis, optical imaging, drug delivery and sensing.[9-11] MOFs as promising materials, have also been used for Fe^{3+} sensing. Most of the current MOF based Fe^{3+} ion sensors use fluorescent sensing approaches.[12-15] Several lanthanide-based MOFs (Ln-MOF) such as Terbium (Tb) and Europium (Eu)-MOF, owing to their unique optical properties, are widely used as fluorescent sensors for Fe^{3+} based on dynamic or static quenching effects.[16-18] However, these MOF-based fluorescent Fe^{3+} ion sensors require expensive fluorescence measurement equipment and complicated operations, which make them difficult to use in resource-constrained environments. Moreover, many current MOF fluorescent sensors are based on bulk MOF materials.[12,17,19] However, the usage of bulk-sized MOFs results in slow signal response due to the relatively small surface area of the interaction between MOFs and metal ions. Moreover, poor stability in aqueous solutions allows bulk-sized MOFs to only sense ions in organic solution but is not suitable for aqueous and biological environment.[20]

Zero-dimensional (0D) nanostructured materials (NSMs) such as semiconductor quantum dots,[21] graphene-like material quantum dots,[22-23] hollow nanospheres[24] and nano-lenses[25] have been used in various biological applications due to their high surface-to-volume ratio, enhanced sensitivity and unique optical properties. Most recently, low-dimensional MOF materials such as 2D MOF nanosheets have raised high interests as new members of 2D nanomaterial family due to its tunable components and flexible structures for various applications.[26] However, to the best of our knowledge, 0D MOF nanomaterials with ultrasmall size under 10 nm have rarely been reported. In this paper, we successfully synthesized 0D Zn-MOF-74 nanodot with an ultrasmall size of 4 nm and developed a simple and label-free colorimetric approach based on ultrasmall Zn-MOF-74 nanodot for highly sensitive and selective Fe^{3+} sensing. The ultra-small size and excellent water dispersibility of this MOF nanodot enable the close contact with target Fe^{3+} ions in aqueous environment, resulting in a low limit of detection of 1.04 μM and a fast response within seconds. A new Fe^{3+} sensing mechanism based on the selective disruption of Zn-MOF-74 coordination structure by Fe^{3+} and the formation of blue-colored Fe-DOBDC complex in aqueous solution was proposed and demonstrated. Unlike fluorescent sensing, this MOF nanodot based colorimetric Fe^{3+} detection can be easily implemented without using an expensive fluorescence spectrometer and laborious manipulation, which may provide an easy and simple approach for metal ion sensing. Finally, the ultrasmall-size nature and highly dispersible and stable nature in aqueous solutions make this Zn-MOF-74 nanodot a potential candidate for Fe^{3+} sensing in environmental and biological systems.

2. EXPERIMENTAL SECTION

2.1 Reagents and Materials

Zinc acetate dihydrate, 2,5-Dihydroxyterephthalic acid (DOBDC) were purchased from Aladdin Chemical Co., Ltd., Shanghai. Ethanol absolute was purchased from International Laboratory USA. N, N-Dimethylformamide (DMF) was purchased from DUKSAN Pure Chemicals, Co. Ltd, South Korea. Nitric acid (Tracemetal Grade) was purchased from Anaqua Chemical Supply Co. Ltd., Hong Kong. Potassium bromide (FT-IR grade), metal nitrates and Zinc standard solution were purchased from Sigma-Aldrich, USA. All the chemicals were used as received without further treatment.

2.2 Synthesis.

Zn based MOF nanodots were prepared based on a method reported by Díaz-García, et al with modifications.[27] Briefly, 30 mL solution containing 0.6 mmol of 2,5-dihydroxyterphthalic acid (DOBDC) in N, N-Dimethylformamide (DMF) was added dropwise over 60 mL DMF solution of Zinc acetate dehydrate (0.1 mM) under stirring. The above mixture was incubated at room temperature for 48 h and followed by rinsing with 40 mL DMF and 40 mL ethanol with centrifugation three times. After ultrasonic treatment for 0.5 h in ice water, the yellow nanocrystal Zn-MOF-74 [$Zn_2(C_8H_2O_6)$] was then collected by filtration (Millipore, 0.22 μm) and dispersed in DI water for further usage.

2.3 Characterization

The transmission electron microscope (TEM) images were collected by a JEOL JEM-2100 F microscope. Zeta potential of the nanodots were obtained using a Malvern ZEN 3600 Zetasizer Nano System. Ultraviolet and visible (UV-vis) absorbance were measured by Ultrospec 2100 Pro

spectrophotometer (Amersham Biosciences). Powder X-ray diffraction (PXRD) patterns were collected at 293 K on a Rigaku SmartLab diffractometer using Cu Kα radiation. Thermogravimetric analysis (TGA) was performed using a Mettler Toledo TGA/DSC3+ instrument at a heating rate of 10 °C/min under N_2 flow. The Fourier transform infrared (FT-IR) spectra were measured in KBr pellets on the Bruker Vertex-70 IR Spectroscopy in the wavelength region of 400 – 4000 cm^{-1}. The determination of the accurate concentration of Zinc and iron was performed by inductively coupled plasma-optical emission spectroscopy (ICP-OES) on Agilent 710 Series ICP Optical Emission Spectrometer.

2.4 Sample preparation for ICP studies.

1 mL (1 mg/mL) solution of MOF nanodots was mixed with 0.5 mL of Fe^{3+} at concentrations of 1 mM to 25 mM. After gently shaking for 5 min, the large MOF nanocrystals were removed by centrifugation at 13500 rpm for 30 min. 0.5 mL of the above filtrate was transferred to a new tube and diluted to 5 mL with nitric acid (Trace metal, 69%) before introduced for ICP measurement. The ICP-OES was calibrated with element standard solution prepared with 1000 ppm Zn standard and 1000 ppm Fe standard by successive dilutions with an HNO_3 5% (w/w) matrix.

2.5 Metal ion sensing

For metal ion colorimetric sensing, 400 μL of 0.1 mg/mL Zn-MOF-74 aqueous solution was mixed with 100 μL of aqueous solution of 13 kinds of metal ions M^{n+} (M= Mg^{2+}, Ca^{2+}, Ni^{2+}, Co^{2+}, Cu^{2+}, Cd^{2+}, Mn^{2+}, Na^{+}, K^{+}, Cr^{3+}, Fe^{2+}, Al^{3+}, Fe^{3+}). After pipetting for several times, the mixture was subjected to the UV-vis spectrometer to record the UV-vis spectrum. The characteristic peak at 600 nm is measured and calibrated for Fe^{3+} quantitative measurement.

3. RESULTS AND DISCUSSION

3.1 Mechanism of Fe^{3+} sensing

Zn-MOF-74 generally features hexagonal structure consisting of connection between Zn^{2+} and DOBDC ligands. The Zn atom is coordinated with DOBDC ligands through carboxyl and hydroxyl groups to form Zn-O bond. This Zn-O bond has a length from 2.02 to 2.18 Å. There are one-dimensional channels about 10.3 × 5.5 $Å^2$ inside the hexagonal structure, which may link with guest molecules. As shown in Scheme 1, with the addition of Fe^{3+}, the higher affinity between exotic Fe^{3+} and phenolic hydroxyl group of DOBDC causes the detachment of DOBDC from Zn^{2+}. The detached DOBDC then combines with Fe^{3+} to form the specific colorimetric substance Fe-DOBDC. Due to the strong absorbance of newly formed Fe-DOBDC salt complex at 600 nm in UV-vis absorbance spectra, the solution color is changed from transparency to blue.

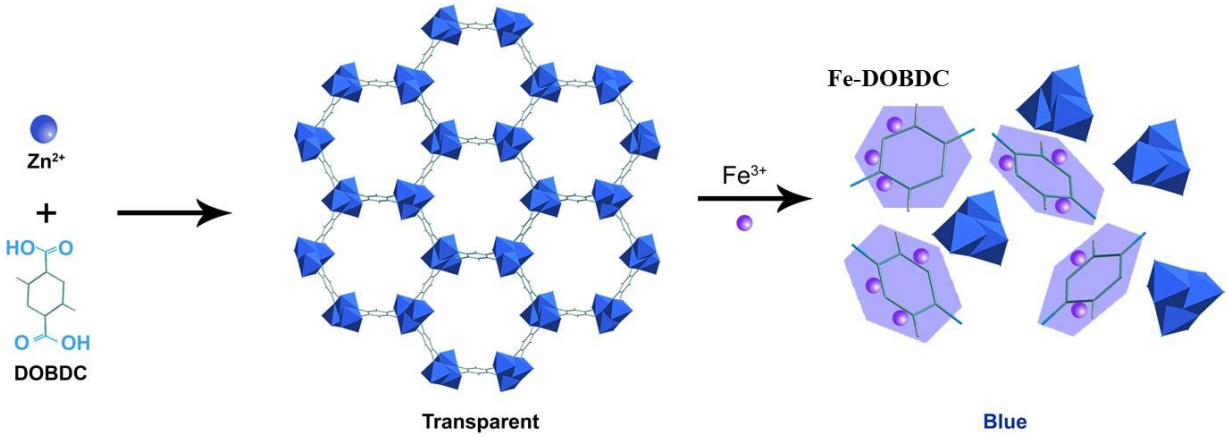

Scheme 1 The schematic illustration for the fabrication of Zn-MOF-74 nanodot and Fe^{3+} sensing.

3.2 Characterization of Zn-MOF-74 ultrasmall nanodot

The synthesis of stable MOF nanocrystals is always challenging. The currently reported nanoszied Zn-MOF-74 crystals are in the range 20-30 nm, which is synthesized with a precipitation approach rather than crystallization process.[27] Here, we attempted to manipulate the synthesis

conditions of this precipitation approach to further downsize Zn-MOF-74 crystal. Generally, MOF formation could be simplified to ligand substitution with metal ions or metal clusters.[28-29] This coordination chemistry could be used to analyze the equilibrium of Zn-MOF-74 formation.[30] For the specific Zn-MOF-74 nanocrystal formation, Zn^{2+} is coordinated with DOBDC ligand through carboxyl and hydroxyl groups to form Zn-MOF-74 monomers Zn_2(DOBDC) (Figure 1a). The equilibrium of Zn-MOF-74 monomers could be represented by Equation 1. Here, Zn-MOF-74 monomer is treated as soluble species with limited scattering, Zn-MOF-74 nanocrystal is formed with the repeating unites of monomer Zn_2(DOBDC) and excessive DOBDC ligand is applied. Therefore, Zn-MOF-74 nanocrystal formation could be summarized by Equation 2.

$$Zn_2 + DOBDC \rightleftharpoons [Zn_2DOBDC]_{monomer} \quad (1)$$

$$[Zn_2DOBDC] = K \times [Zn_2DOBDC]_{monomer} \times [DOBDC] \quad (2)$$

Generally, the manipulation of factors in Equation 2 such as the concentration of Zn_2(DOBDC) monomer and DOBDC ligand would eventually affect the particle size through the nucleation process. Here, we downsize Zn-MOF-74 by diluting the system with low metal ion concentration aiming to generate relatively more Zn_2(DOBDC) monomers with smaller size.

Transmission electron microscopy (TEM) was used to characterize the morphology of the synthesized Zn-MOF-74 nanodots. As shown in Figure 1b, the synthesized MOF nanodots at room temperature showed good water dispersity. Sonication of synthesized MOF nanodots led to colloidal suspension, which showed a typical Tyndall effect (Figure 1b inset). The particle size distribution of MOF nanodts ranges from 2 to 5.5 nm and the average particle size is about 4.0 nm (Figure 1c), which is much smaller than that of the previously reported Zn-MOF-74 nanoparticles (20 to 50 nm).[27] High-resolution TEM (HRTEM) image indicated the high crystallinity of

synthesized MOF nanodots with the lattice fringe around 0.207 nm (Figure 1d inset), which could be assigned to [110] plane of Zn-MOF-74. The prepared MOF nanodot solution showed good transparency after one week standing, which demonstrated the long-term water stability (Figure S1).

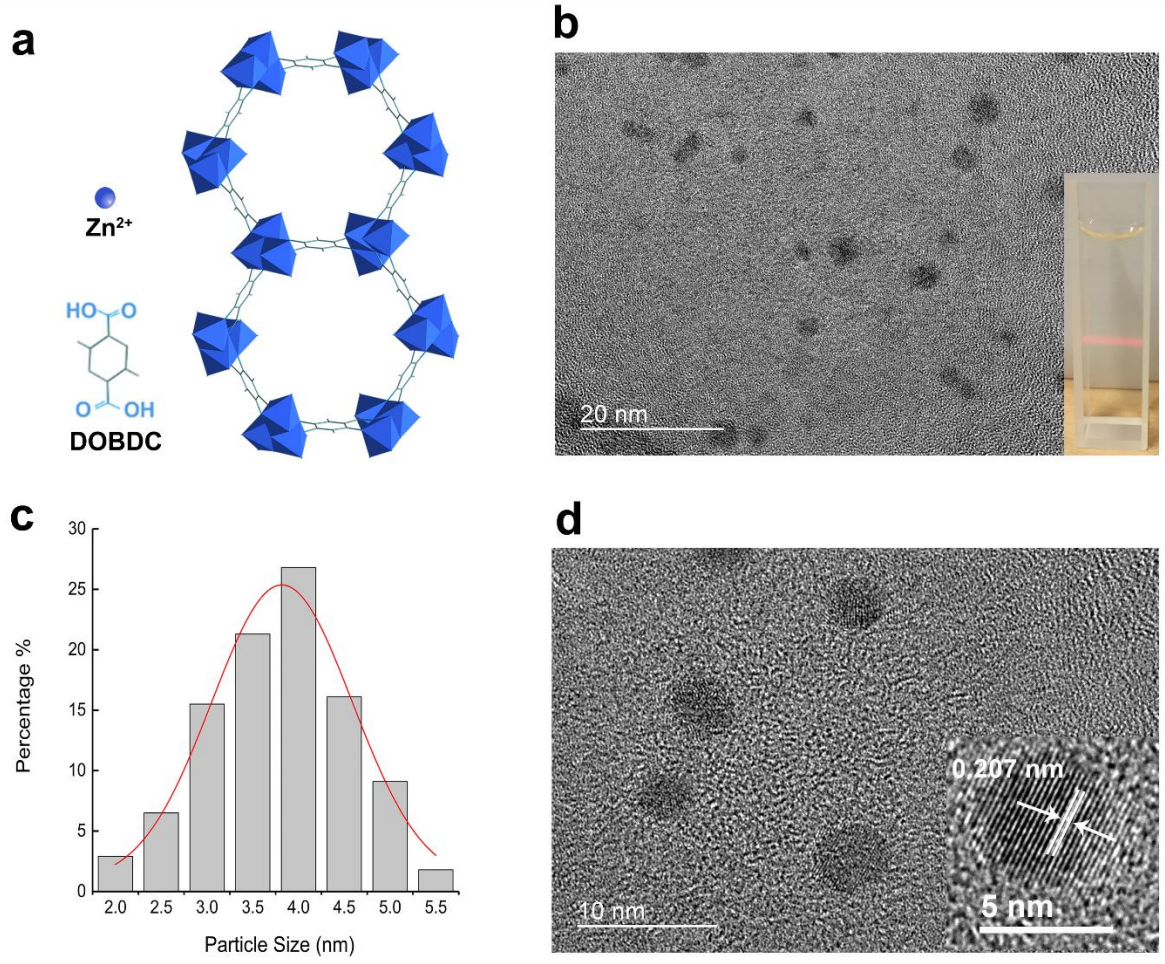

Figure 1 (a) Schematic architecture of the Zn-MOF-74. (b) Transmission electron microscopy (TEM) image of Zn-MOF-74 nanodot. (c) Size distribution of Zn-MOF-74 nanodots. (d) High resolution Transmission electron microscopy (HRTEM) image of Zn-MOF-74 nanodots

Powder X-ray diffraction (XRD) was used to further determine the crystallinity of Zn-MOF-74 nanodots. The XRD pattern of as-synthesized MOF nanodots registered with 2θ steps of 0.01° was agreed well with the simulated curve (Figure 2a). The peaks of XRD pattern at ~6.8° and ~11.6° indicated the [110] and [300] reflections of Zn-MOF-74 crystals, respectively. Zeta potential analysis was also carried out to determine the surface charge of Zn-MOF-74 nanodots. Figure S2 showed that Zeta potential of Zn-MOF-74 nanodot was -18 mV, indicating that Zn-MOF-74 was physically stable in the aqueous solution. This negatively charged surface allowed the MOF nanodots to be well dispersed in the aqueous solution for various biological applications. The surface chemistry of Zn-MOF-74 nanodot was then investigated by FTIR Spectroscopy. Characteristic stretching vibrations of the coordinating carboxylate groups were observed at 1558 cm^{-1}, 1450 cm^{-1}, 1409 cm^{-1}, respectively. The transmittance at ~920 cm^{-1} could be ascribed to the -OH group (Figure S3). The outstanding transmittance peak at 480 cm^{-1} represented the Zn-O bond in MOF nanodot compared to that of DOBDC ligand, indicating the formation of Zn-MOF-74 framework (Figure S3). The as-prepared MOF nanodots were also analyzed by thermogravimetric analysis (TGA) (Figure 2b). The TGA diagram demonstrated that MOF nanodots had high thermal stability up to 400 °C. The first step of weight loss around 39% in the region of 50~ 120 °C indicated the removal of water and DMF molecules in the pores of MOF structure. The second step of weight loss around 50% occurred after 400 °C, which suggested the decomposition of MOF structure. The porosity of Zn-MOF-74 was analyzed by nitrogen adsorption–desorption isotherms and the Brunauer–Emmett–Teller (BET) surface area was calculated to be 314.6 m^2 g^{-1} (Figure S4).

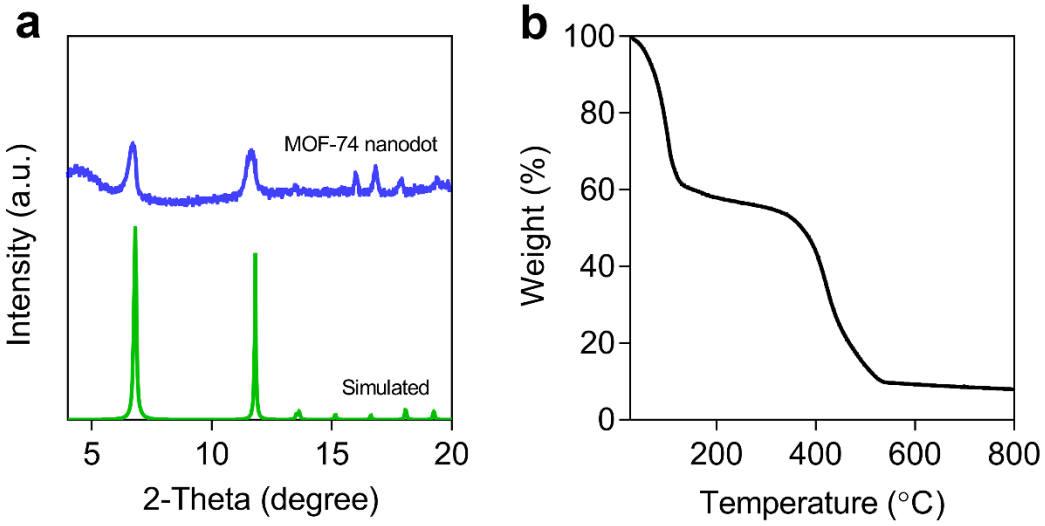

Figure 2 (a) Powder XRD pattern of simulated MOF-74 and as-synthesized MOF nanodots. (b) Thermogravimetric analysis (TGA) for the MOF nanodots.

3.3 Fe^{3+} ion detection

Because of its highly dispersive nature and ultra-small size, this MOF nanodot has high surface area available for the reaction with metal ions, making the synthesized ultrasmall Zn-MOF-74 nanodots a good candidate for metal ion sensing in aqueous environment. The synthesized Zn-MOF-74 nanodots were then used for Fe^{3+} ion detection in aqueous solution. Figure 3a showed the UV-visible absorption spectra of solution with Zn-MOF-74 nanodots before and after addition of Fe^{3+} ion. Before the addition of Fe^{3+}, Zn-MOF-74 nanodots showed an absorption peak at 352 nm in the UV-Vis spectrum. With the addition of Fe^{3+} ion, Zn-MOF-74 nanodots showed a new peak at 600 nm. This red shift was also observed as a color change from transparency to blue for MOF nanodots with addition of Fe^{3+} within seconds (Figure 3b). The solution color and the UV-vis absorption spectra were quickly, significantly and selectively changed when Zn-MOF-74 nanodot solution was mixed with the Fe^{3+} in aqueous environment, which indicated the possibility of colorimetric sensing of Fe^{3+} ion in aqueous solution.

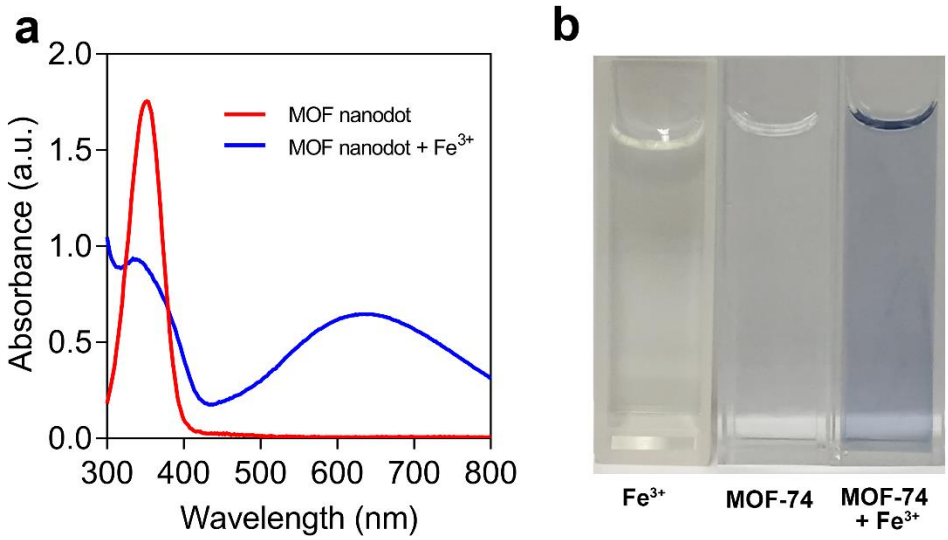

Figure 3 (a) UV-vis absorbance spectra of MOF nanodots and MOF nanodots with Fe^{3+}. (b) The color change of the MOF nanodots after the addition of Fe^{3+}.

The amplitude of UV-Vis spectra at 600 nm of MOF-74 nanodot solution gradually increased as the concentration of Fe^{3+} added into MOF-74 nanodot solution increased (Figure S5). Moreover, the amplitude of the absorption peak of 600 nm showed a highly broad linear relationship with the concentration of Fe^{3+} up to 1250 μM expressed as an equation of y = 0.01525+0.00168 x and R^2=0.99727, where y is the amplitude of characteristic peak 600 nm and x is the concentration of Fe^{3+} (Figure 4). The other reported sensors for Fe^{3+} detection are generally within 500 μM of Fe^{3+}.[31-33] Moreover, the limit of detection (LOD) of this Zn-MOF-74 nanodot based sensor reached 1.04 μM of Fe^{3+}, which was calculated based on the control signal plus 3 times of standard deviation. The LOD of this MOF nanodot sensor is comparable with those of fluorescent-based sensing methods ranging from 0.45 μM to hundreds of micromoles (Table 1), but with much simpler instrumentation and even naked-eye recognition. The Fe^{3+} sensing was also tested in aqueous solution with different pH values. The experimental results showed that this MOF nanodot

based sensor showed good pH stability and was able to detect Fe^{3+} in both weak acid and base solution (Figure S6).

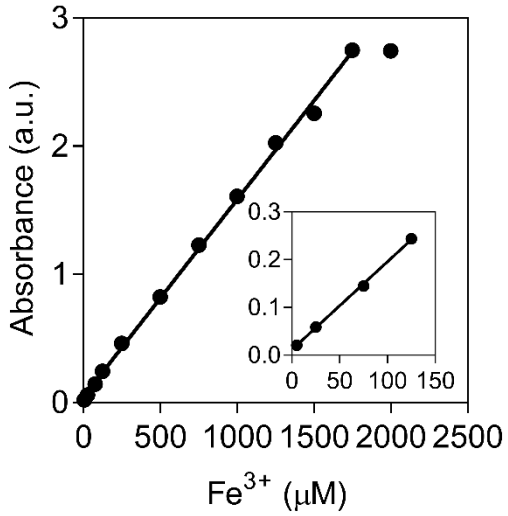

Figure 4 The fitting curve of the UV-vis absorbance of MOF nanodots versus Fe^{3+} concentration (linear range 1~1250 μM).

Table 1. Comparison of Fe^{3+} sensors based on various materials

Material	Technique	LOD (μM)	Linear detection range	Ref.
MIL-53 (Al)	Fluorescent	0.9	3~200 μM	15
Bis(rhodamine)	Fluorescent	50	150~237.5 μM	34
Graphene oxide	Fluorescent	0.64	N/A	35
[Tb(BTB)(DMF)]	Fluorescent	10	10~1000 μM	36
$Eu(C_{22}H_{14}O_2)_3$	Fluorescent	100	0.1~5 mM	31
$Eu(C_{33}H_{24}O_{12})(H_2NMe)(H_2O)$	Fluorescent	200	N/A	18
Salicylaldehyde-azine (SA)	colorimetric	9.5	15.7~23.6 μM	37
Carbon Dots	colorimetric	0.3	0.3~546 μM	38
Bis-rhodamine Urea	colorimetric	4.3	30~70 μM	39
Our work	colorimetric	1.04	1-1250 μM	

To evaluate the selectivity of MOF nanodots to various metal ions, the absorption spectra of MOF nanodot solution (400 μL, 0.1mM) mixed with 13 different kinds of aqueous metal ions (0.1

mM) were taken including Mg^{2+}, Ca^{2+}, Ni^{2+}, Co^{2+}, Cu^{2+}, Cd^{2+}, Mn^{2+}, Na^{+}, K^{+}, Fe^{2+}, Cr^{3+}, Al^{3+} and Fe^{3+}. The UV-vis absorption spectra did not show obvious changes between 420 and 700 nm for other metal ions except for Fe^{3+} (Figure 5a). In contrast, there was a significant increase in the region of 420 – 800 nm, peaking at around 600 nm with the addition of Fe^{3+}. The amplitudes of characteristic 600 nm for all metal ions were shown in Figure 5b. it is obvious that the amplitude of Fe^{3+} ions is around 7 folds higher than other metal ions. Moreover, the color of the MOF nanodot solution did not change with the addition of metal ions except for the addition of Fe^{3+}, which induced a color change to blue. We further added Zn^{2+} into the Fe-DOBDC solution to evaluate whether this MOF-74 nanodot based Fe^{3+} colorimetric sensing was reversible. As shown in the UV-Vis spectra (Figure S7), the addition of Zn^{2+} (0.1 mM) caused a slight shift of absorption peak of Fe-DOBDC, which still showed a strong absorption peak around 580 nm~600 nm. This experiment demonstrated the MOF-74 nanodot based colorimetric sensing of Fe^{3+} was not reversible.

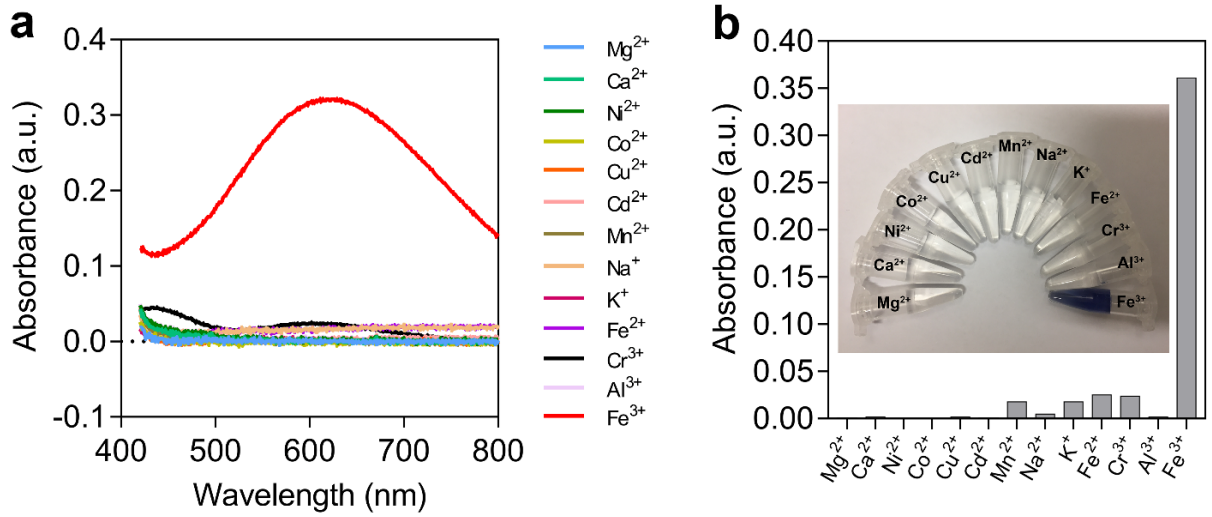

Figure 5 (a) UV-vis absorbance spectra of MOF nanodots with 50 μM of different metal ions. (b) Amplitude of characteristic 600 nm peak of MOF nanodots in UV-vis absorbance spectra with different metal ions. The inset shows the color change of MOF nanodots with metal ions in aqueous solution.

3.4 Colorimetric sensing mechanism exploration

As shown in Scheme 1, it is hypothesized that the addition of Fe^{3+} will lead to 1) the collapse of Zn-MOF-74 structure by the formation of Fe-DOBDC complex and release of free Zn^{2+} ions in solution; 2) the solution color changed from transparency to blue due to the generated Fe-DOBDC complex. To demonstrate the first hypothesis, powder XRD was firstly performed with solution of Zn-MOF-74 nanodots before and after addition of Fe^{3+}. As shown in Figure 6a, powder XRD spectrum of addition of Fe^{3+} led to the disappearance of the characteristic peaks of Zn-MOF-74 at ~6.8° and ~11.6° compared with that of original curve, indicating the collapse of the MOF structure upon the addition of Fe^{3+}. Moreover, we also observed that the characteristic peaks in powder XRD pattern gradually disappeared with the increasing amount of Fe^{3+} up to 50 mM, which demonstrated the gradual disruption of the metal-organic framework by Fe^{3+} (Figure S8). Other metal ions did not show any change in XRD patterns, indicating no disruption of MOF structure (Figure S9).

FTIR spectra were also measured to monitor the formation of Fe-DOBDC complex. As shown in Figure 6b, a strong peak at 578 cm^{-1} was observed after the addition of Fe^{3+}, which could be ascribed to the formation of Fe-O bond due to the coordination of Fe^{3+} with hydroxyl groups on the DOBDC. As both hydroxyl and carboxyl groups were coordinated with Zn atoms in the framework structure, the high affinity between exotic Fe^{3+} and phenolic hydroxyl groups might cause the detachment of ligands from Zn^{2+} atoms and form an iron (III)-phenol salt complex: Fe-DOBDC.[40,41] XPS spectra were also measured to demonstrate the formation of Fe-DOBDC complex (Figure S10). A shift of Fe2p peak from 711.3 eV to 712.1 eV was observed after addition of Fe^{3+} in MOF-74 solution. The slight increase of binding energy of Fe2p is due to the formation of Fe-O bond of Fe-DOBDC. To verify this hypothesis of release of free Zn^{2+} upon addition of

Fe^{3+}, inductively coupled plasma optical emission spectrometry (ICP-OES) was used to analyze the concentration of released Zn element in the supernate of MOF nanodot solution after the addition of Fe^{3+}. The ICP results showed a significant increase of free Zn element from 26.3 to 223.2 ppm when the amount of Fe^{3+} increased from 1 mM to 25 mM (Figure 6c). The above results confirmed our first hypothesis that the structure of metal-organic framework was collapsed with the addition of Fe^{3+} due to the formation of Fe-DOBDC complex and release of free Zn^{2+} ions in solution in aqueous environment.

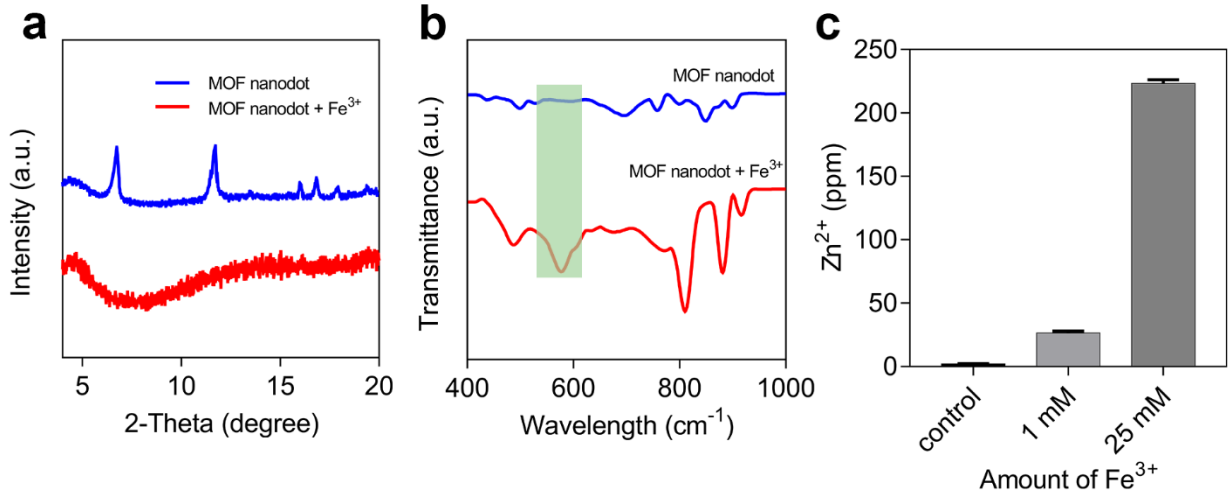

Figure 6 Powder XRD pattern (a) and FT-IR spectra (b) of MOF nanodots with/without 25 mM of Fe^{3+}. (c) Free Zn ions in the MOF nanodots solution after the addition of different amount of Fe^{3+} measured by ICP-OES.

We further investigated whether the increase of absorbance at ~600 nm was due to the newly formed Fe-DOBDC complex. The disruption process of Zn-MOF-74 structure with addition of Fe^{3+} can be expressed as the following Equation 3.

$$Fe^{3+} + [Zn_2DOBDC]_{MOF} \rightarrow [Fe - DOBDC]_{complex} + Zn^{2+} \qquad (3)$$

The strong affinity between Fe^{3+} and DOBDC ligand leads to the disruption of Zn-MOF-74 structure, followed by the formation of Fe-DOBDC complex and the release of free Zn ions. The material components in the Zn-MOF-74 nanodot solution after addition of Fe^{3+} possibly include the residual Zn-MOF-74 nanodot, Fe^{3+} ion, Fe-DOBDC complex and free Zn^{2+}. Figure 7 shows the UV-Vis absorption spectra for solutions of Zn-MOF-74 nanodot, Fe^{3+} ion, Fe-DOBDC complex and Zn^{2+} ion. It is clearly observed that only Fe-DOBDC complex showed a significant peak around 600 nm. Other material components such as Fe^{3+} ion, Zn-MOF-74 nanodot and Zn^{2+} ion did not show obvious peaks in the visible color range of 420 – 800 nm. Correspondently, the tube with Fe-DOBDC shows blue color and those with Fe^{3+} ion, Zn-MOF-74 nanodot and Zn^{2+} ion show transparency (Figure 7 inset). The above results demonstrated our hypothesis that the solution color change from transparency to blue was due to the generated Fe-DOBDC complex. Based on the above experiments and results, we could conclude that the change of color and absorbance of Zn-MOF-74 nanodot upon the addition of Fe^{3+} is attributed to the ligand dissociation from MOF and phenolic iron complex produced by the interaction between ligand and Fe^{3+}.

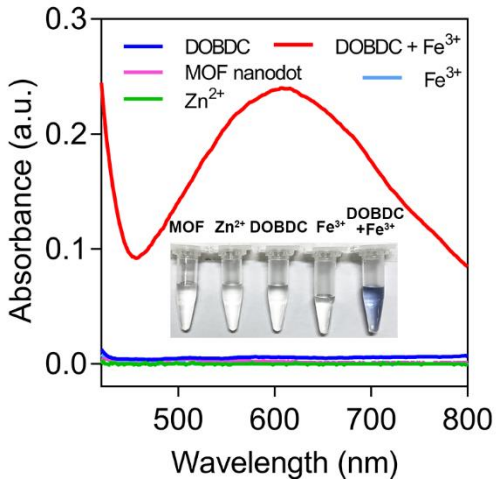

Figure 7 UV-Vis spectra of possible material components in the solution of disrupted Zn-MOF-74 nanodots with addition of Fe^{3+} (Fe-DOBDC, DOBDC, Zn-MOF-74, Zn^{2+} and Fe^{3+})

4. CONCLUSION

In this work, we successfully downsized Zn-MOF-74 nanoparticles within 5 nm by manipulating the initial conditions with a diluted material system. The usage of bulk-sized MOF material might lead to a slow response with a relative small surface reaction area for Fe^{3+} sensing. Moreover, bulk-sized MOF material has poor stability in aqueous solution, which is lack of capability for Fe^{3+} detection in aqueous environment. The synthesized ultrasmall Zn-MOF-74 nanodots were then used for rapid and sensitive detection of Fe^{3+} ions in aqueous solution. Due to its ultrasmall size and high dispersity in aqueous solution, MOF nanodots provide large surface area available for reaction, leading to a high sensitivity, broad liner detection range, and rapid response for Fe^{3+} ion sensing. The selectivity of this MOF nanodot based sensor for Fe^{3+} ion detection was also demonstrated compared with other common metal ions. Finally, we demonstrated that the selective Fe^{3+} sensing mechanism is dependent on selective framework structure collapse and the formation of Fe-DOBDC complex with blue color. The highly dispersive and ultrasmall size may provide other possibilities for Fe^{3+} sensing in the biological systems.

ASSOCIATED CONTENT

Supporting Information

The Supporting Information is available free of charge on the ACS Publications website.

Stability in aqueous solution of MOF nanodots; Zeta potential curve of Zn-MOF-74 nanodots; FT-IR spectra of MOF nanodots and DOBDC ligands; Stability of Fe^{3+} sensing at different pH values; Powder XRD pattern of MOF nanodots; Comparison of powder XRD patterns of MOF nanodots with addition of 25 mM of various ions (PDF)

AUTHOR INFORMATION

Corresponding Authors

Phone +852-27664946; Fax +852- 23342429; E-mail: Mo.Yang@polyu.edu.hk (MY)

ORCID

Mo Yang: 0000-0002-3863-8187

Jiuhai Wang: 0000-0003-3845-9901

Notes

The authors declare no competing financial interest.

ACKNOWLEDGMENT

This work was supported by the National Natural Science Foundation of China (NSFC) (Grant No. 81471747 and 31771077), the Hong Kong Research Council General Research Grant (PolyU 152169/17E) and the Hong Kong Polytechnic University Internal Fund (1-ZVJ7 and 1-YW1L). Guang dong-Hong Kong Technology Cooperation Funding Scheme (2016A050503027). This work was also supported by the University Research Facility in Life Sciences of the Hong Kong Polytechnic University.

ABBREVIATIONS

MOF: metal-organic framework; ICP-MS: inductively coupled plasma mass spectrometry; DOBDC: 2,5-dihydroxyterephthalic acid; NSM: nanostructured materials.

REFERENCE

(1) Hider, R. C.; Kong, X. L. Iron Speciation in the Cytosol: An Overview. *Dalton Trans.* **2013**, *42*, 3220-3229.

(2) Carter, K. P.; Young, A. M.; Palmer, A. E. Fluorescent Sensors for Measuring Metal Ions in Living Systems. *Chem. Rev.* **2014**, *114*, 4564–4601.

(3) Bakkaus, E.; Collins, R. N.; Morel, J. L.; Gouget, B. Anion Exchange Liquid Chromatography-Inductively Coupled Plasma-Mass Spectrometry Detection of the Co^{2+}, Cu^{2+}, Fe^{3+} and Ni^{2+} Complexes of Mugineic and Deoxymugineic Acid. *J. Chromatogr. A* **2006**, 1129, 208-215.

(4) Arnold, G. L.; Weyer, S.; Anbar, A. D. Fe Isotope Variations in Natural Materials Measured Using High Mass Resolution Multiple Collector ICPMS. *Anal. Chem.*, **2004**, *76*, 322–327.

(5) Andersen, J. E. T. A Novel Method for the Filterless Preconcentration of Iron. *Analyst* **2005**, *130*, 385–390.

(6) Yaghi, O. M.; Li, H. L. Hydrothermal Synthesis of a Metal-Organic Framework Containing Large Rectangular Channels. *J. Am. Chem. Soc.* **1995**, *117*, 10401–10402.

(7) Liu, W.; Huang, J.; Yang, Q.; Wang, S.; Sun, X.; Zhang, W.; Liu, J.; Huo, F. Multi-Shelled Hollow Metal-Organic Frameworks. *Angew. Chem. Int. Ed.* **2017**, *56*, 5512–5516.

(8) Lu, G.; Li, S.; Guo, Z.; Farha, O. K.; Hauser,B. G.; Qi, X.; Wang, Y.; Wang, X.; Han, S.; Liu, X.; DuChene, J. S.; Zhang, H.; Zhang, Q.; Chen, X.; Ma, J.; Loo, S. C.; Wei, W. D.; Yang, Y.; Hupp, J. T.; Huo, F. Imparting Functionality to A Metal-Organic Framework Material by Controlled Nanoparticle Encapsulation. *Nat. Chem.* **2012**, *4*, 310–316.

(9) Cui, Y. J.; Li, B.; He, H. J.; Zhou, W.; Chen, B. L.; Qian, G. D. Metal-Organic Frameworks as Platforms for Functional Materials. *Acc. Chem. Res.* **2016**, *49*, 483–493.

(10) Chen, Y. Z.; Wang, Z. U.; Wang, H. W.; Lu, J. L.; Yu, S. H.; Jiang, H. L. Singlet Oxygen-Engaged Selective Photo-Oxidation over Pt Nanocrystals/Porphyrinic MOF: The Roles of Photothermal Effect and Pt Electronic State. *J. Am. Chem. Soc.* **2017**, *139*, 2035–2044.

(11) Wang, W. Q.; Wang, L.; Li, Y.; Liu, S.; Xie, Z. G.; Jing, X. B. Nanoscale Polymer Metal-Organic Framework Hybrids for Effective Photothermal Therapy of Colon Cancers. *Adv. Mater*. **2016**, *28*, 9320–9325.

(12) Zhou, Y.; Chen, H.H.; Yan, B. An Eu^{3+} Post-Functionalized Nanosized Metal-Organic Framework for Cation Exchange-Based Fe^{3+}-Sensing in an Aqueous Environment. *J. Mater. Chem. A* **2014**, *2*, 13691–13697.

(13) Xu, H.; Gao, J.; Qian, X.; Wang, J.; He, H.; Cui, Y.; Yang, Y.; Wang, Z.; Qian, G. Metal-Organic Framework Nanosheets for Fast-Response and Highly Sensitive Luminescent Sensing of Fe^{3+}. *J. Mater. Chem. A* **2016**, *4*, 10900–10905.

(14) Wang, J.; Jiang, M.; Yan, L.; Peng, R.; Huangfu, M.J.; Guo, X. X. Li, Y.; Wu, P. Y., Multifunctional Luminescent Eu(III)-Based Metal-Organic Framework for Sensing Methanol and Detection and Adsorption of Fe(III) Ions in Aqueous Solution. *Inorg. Chem.* **2016**, *55*, 12660–12668.

(15) Yang, C. X.; Ren, H. B.; Yan, X. P. Fluorescent Metal-Organic Framework MIL-53 (Al) for Highly Selective and Sensitive Detection of Fe^{3+} in Aqueous Solution. *Anal. Chem.* **2013**, *85*, 7441–7446.

(16) Cui, Y.; Yue, Y.; Qian, G.; Chen, B. Luminescent Functional Metal-Organic Frameworks. *Chem. Rev.* **2012**, *112*, 1126–1162.

(17) Cao, L. H.; Shi, F.; Zhang, W. M.; Zang, S. Q.; Mak, T. C. W. Selective Sensing of Fe^{3+} and Al^{3+} Ions and Detection of 2,4,6-Trinitrophenol by a Water-stable Terbium-Based Metal-Organic Framework. *Chem. Eur. J.* **2015**, *21*, 15705–15712.

(18) Dang, S.; Ma, E.; Sun, Z. M.; Zhang, H. J. A Layer-Structured Eu-MOF as a Highly Selective Fluorescent Probe for Fe^{3+} Detection Through a Cation-Exchange Approach. *J. Mater. Chem.* **2012**, *22*, 16920–16926.

(19) Zhou, J. M.; Shi, W.; Li, H. M.; Li, H.; Cheng, P. Experimental Studies and Mechanism Analysis of High-Sensitivity Luminescent Sensing of Pollutional Small Molecules and Ions in Ln_4O_4 Cluster Based Microporous Metal-Organic Frameworks. *J. Phys. Chem. C* **2013**, *118*, 416–426.

(20) Rosenthal, S. J.; Chang, J. C.; Kovtun, O., McBride, J. R.; Tomlinson, I. D. Biocompatible Quantum Dots for Biological Applications. *Chem. Biol.* **2011**, *18*, 10–24.

(21) Dong, X. Y.; Wang, R.; Wang, J. Z.; Zang, S. Q.; Mak, T. C. W. Highly selective Fe^{3+} sensing and proton conduction in a water-stable sulfonate-carboxylate Tb-organic-framework. *J. Mater. Chem. A* **2015,** *3*, 641-647.

(22) Dong, H.; Tang, S.; Hao, Y.; Yu, H.; Dai, W.; Zhao, G.; Cao, Y.; Lu, H.; Zhang, X,; Ju, H. Fluorescent MoS_2 Quantum Dots: Ultrasonic Preparation, Up-Conversion and Down-Conversion Bioimaging, and Photodynamic Therapy. *ACS Appl. Mater. Interfaces* **2016**, *8*, 3107–3114.

(23) Zhu, J.; Tang, J.; Zhao, L.; Zhou, X.; Wang, Y.; Yu, C. Ultrasmall, Well-Dispersed, Hollow Siliceous Spheres with Enhanced Endocytosis Properties. *Small* **2010**, *6*, 276–282.

(24) Lee, J. Y.; Hong, B. H.; Kim, W. Y.; Min; S. K.; Kim, Y.; Jouravlev, M. V.; Bose, R.; Kim, K. S.; Hwang, I. C.; Kaufman, L. J.; Wong, C.W.; Kim, P.; Kim, K. Near-Field Focusing

and Magnification Through Self-Assenbled Nanoscale Spherical Lenses. *Nature* **2009**, *460*, 498–501.

(25) Peng, Y.; Li, Y.; Ban, Y.; Jin, H.; Jiao, W.; Liu, X.; Yang, W. Metal-Organic Framewok Nanosheets as Building Blocks for Molecular Sieving Membranes. *Science* **2014**, 346, 1356–1359.

(26) Peng, Y.; Li, Y.; Ban, Y.; Yang, W. Two-Dimensional Metal-Organic Framework Nanosheets for Membrane-Based Gas Separation. *Angew. Chem. Int. Ed.* **2017**, 56, 9757–9761.

(27) Diaz-Garcia, M.; Mayoral, A.; Diaz, I.; Sanchez-Sanchez, M. Nanoscaled M-MOF-74 Materials Prepared at Room Temperature. *Cryst. Growth Des.* **2014**, *14*, 2479–2487.

(28) Feng, D.; Wang, K.; Wei, Z.; Chen, Y.-P.; Simon, C. M.; Arvapally, R. K.; Martin, R. L.; Bosch, M.; Liu, T.-F.; Fordham, S.; Yuan, D.; Omary, M. A.; Haranczyk, M.; Smit, B.; Zhou, H.-C. Kinetically Tuned Dimensional Augmentation as a Versatile Synthetic Route Towards Robust Metal-Organic Frameworks. *Nat. Commun.* **2014**, *5*, 5723.

(29) Park, J.; Jiang, Q.; Feng, D.; Mao, L.; Zhou, H. C. Size-Controlled Synthesis of Porphyrinic Metal-Organic Framework and Functionalization for Targeted Photodynamic Therapy. *J. Am. Chem. Soc.* **2016**, 138, 3518–3525.

(30) Tang, Q.; Liu, S. X.; Liu, Y. W.; Miao, J.; Li, S. J.; Zhang, L.; Shi, Z.; Zheng, Z. P. Cation Sensing by a Luminescent Metal-Organic Framework with Multiple Lewis Basic Sites. *Inorg. Chem.* **2013**, *52*, 2799–2801.

(31) Zheng, M.; Tan, H. Q.; Xie, Z. G.; Zhang, L. G.; Jing, X. B.; Sun, Z. C. Fast Response and High Sensitivity Europium Metal Organic Framework Fluorescent Probe with Chelating Terpyridine Sites for Fe^{3+}. *ACS Appl. Mater. Interfaces* **2013**, *5*, 1078–1083.

(32) Chen, Z.; Sun, Y.; Zhang, L.; Sun, D.; Liu, F.; Meng, Q.; Wang, R.; Sun, D. A tubular europium-organic framework exhibiting selective sensing of Fe^{3+} and Al^{3+} over mixed metal ions. *Chem. Commun.* **2013,** *49*, 11557-11559.

(33) Wang, R.; Dong, X. Y.; Xu, H.; Pei, R. B.; Ma, M. L.; Zang, S. Q.; Hou, H. W.; Mak, T. C. W. A super water-stable europium-organic framework: guests inducing low-humidity proton conduction and sensing of metal ions. *Chem. Commun.* **2014,** *50*, 9153-9156.

(34) Weerasinghe, A. J.; Schmiesing, C.; Varaganti, S.; Ramakrishna, G.; Sinn, E. Single- and Multiphoton Turn-On Fluorescent Fe^{3+} Sensors Based on Bis(rhodamine). *J. Phys. Chem. B* **2010,** *114*, 9413-9419.

(35) Mei, Q.; Zhang, Z. Photoluminescent Graphene Oxide Ink to Print Sensors onto Microporous Membranes for Versatile Visualization Bioassays. *Angew. Chem. Int. Ed.* **2012,** *51*, 5602-5606.

(36) Xu, H.; Hu, H.-C.; Cao, C.-S.; Zhao, B. Lanthanide Organic Framework as a Regenerable Luminescent Probe for Fe^{3+}. *Inorg. Chem.* **2015,** *54*, 4585-4587.

(37) Narayanaswamy, N.; Govindaraju, T. Aldazine-based colorimetric sensors for Cu2+ and Fe^{3+}. *Sensors Actuators B: Chem.* **2012,** *161*, 304-310.

(38) Liu, Y.; Duan, W.; Song, W.; Liu, J.; Ren, C.; Wu, J.; Liu, D.; Chen, H. Red Emission B, N, S-co-Doped Carbon Dots for Colorimetric and Fluorescent Dual Mode Detection of Fe3+ Ions in Complex Biological Fluids and Living Cells. *ACS Appl. Mater. Interfaces* **2017,** *9*, 12663-12672.

(39) He, L.; Liu, C.; Xin, J. H. A Novel Turn-on Colorimetric and Fluorescent Sensor for Fe^{3+} and Al^{3+} with Solvent-dependent Binding Properties and Its Sequential Response to Carbonate. *Sensors Actuators B: Chem.* **2015,** *213*, 181-187.

(40) Banerjee, S.; Haldar, B. C. Constitution of Ferri-Phenol Complex in Solution. *Nature* **1950**, *165*, 1012.

(41) Jabalpurwala, K. E.; Milburn, R. M. Iron(III)-Phenol Complexes. II. Iron(III) and Proton Associations with Some Singly Substituted Phenolate Ions at 25°. *J. Am. Chem. Soc.* **1966**, *88*, 3224–3227.

TOC